ENHANCED PHOTOCATALYTIC PROPERTY OF NANO-ZrO_2-SnO_2 NPs FOR PHOTODEGRADATION OF AN AZO DYE

S. AGHABEYGI[*], Z. SHARIFI , N. MOLAHASANI
Department of Chemistry, East Tehran Branch, Islamic Azad University, P O Box 1343986941 Tehran, Iran

The ZrO_2-SnO_2 core-shell NPs was synthesized by hydrothermal method in two steps involving preparation of ZrO_2 core by sol – gel under ultrasonic irradiation and SnO_2 shell layer was covered on core ZrO_2 for preparation of ZrO_2-SnO_2 core-shell The synthesized nano-ZrO_2 and ZrO_2-SnO_2 core-shell NPs were characterized by X-ray powder diffraction (XRD), Fourier transform infrared spectroscopy (FT-IR), Field emission scanning electron microscopy (FESEM) and Emission X-ray dispersive analyses (EDX) . Structural characterization by XRD confirmed the formation of monoclinic ZrO_2 and high crystalline tetragonal tin dioxide. The photo-catalytic activities of nano-ZrO_2 and ZrO_2-SnO_2 core-shell NPs were evaluated by the photo-degradation of Congo red (CR) as an azo dye. The very high efficiency of degradation of CR could be seen on the ZrO_2-SnO_2core-shell photocatalyst, it approaches to 96% after 30 min. Only a slight decrease in the photo-degradation was observed after 3 cycles of the photo- catalysis experiment.

1. Introduction

The removal of various toxic dyes from the textile industry is considered the main cause of water pollution. Congo red is one of the famous dyes that involved extensively as azo dye in textiles industry owing to its high stability. Therefore, the removal of this toxic dye is considered one of the important challenges in the recent years using simple and low costs process [1–4]. The degradation of organic pollutants in water by photo-catalysis, using semiconductors, such as ZnO, ZrO2, SnO2 and so on, has attracted extensive attention during recent 20 years. The application of semiconductors as photocatalyst in photodegradation reaction is a technique to increase the rate of process. The semiconductors can increase the degradation of most kinds of persistent organic pollutants, such as detergents, dyes and pesticides, under UV-light irradiation [5, 6].

.Zirconium dioxide is an n-type semiconductor with band-gap energy of about 5.0 eV that used as heterogeneous catalyst. The values range of band-gap energy is reported between 3.25 and 5.6 eV depending on the preparation technique of the sample and the most frequent and accepted value is 5.0 eV. The CB and VB potentials of it is −1.0 and +4.0 V versus NHE, respectively, allowing its use as a photocatalyst [7, 8]. Tin dioxide is a semiconductor with band-gap energy of about 3.65 eV and it is an n-type semiconductor crystallizing in tetragonal rutile structure and suitable for various applications. The composites of SnO2 have been studied as promising semiconductors in the photocatalytic degradation of wastewaters Tin (IV) oxide has been a widely studied material because of its wide range of applications as gas sensors, heat mirrors, and transparent electrodes for solar cells and in catalysis [9, 10].It is of great interest to improve the photocatalytic activity of semiconductors for the degradation process Mixed semiconductors can often be more efficient photo-catalysts than pure substances. [11]. Combining some semiconductors with different band gaps to form hetero-junctions in photocatalytic systems has become a primary focus of researchers in recent year because of their somewhat unique properties not existed in the individual nano-material arising from the interfacial interaction at the nanoscale [12–17].Various methods, including sol– gel, molten-salt synthesis, microwave technique,

---

[*]Corresponding author: saghabeygi@yahoo.com

chemical precipitation, laser- ablation synthesis, hydrothermal method, emulsion process and sono-chemical have been developed to synthesize SnO2 and ZrO2 nanoparticles [18 - 33] .

The aim of this paper is to study the effect of SnO_2 shell on the structure and morphology of ZrO2-SnO2 core-shell NPs, and its effect on the photo-catalytic activity of it.

2. Experimental work

2.1 Sono-synthesis of ZrO_2

2.4g $ZrCl_4$ was dissolved in 2-propanol (50ml) to get a precursor solution 5 ml of H_2O_2 (%30 v/v) was then dropped into the precursor solution under stirring. The pH of mixture was adjusted 9 by adding ammonium solution until Zirconium gel ($Zr(OH)_4$) was prepared. After aging and stirring for 2days the ZrO_2 gel was placed under probe of ultrasonic irradiation for 30 min. After filtrating the Zirconium gel and calcination of it at 500 °C for 5 h, the white powder of nano ZrO_2 was produced.[30]

2.2 Preparation of nano- ZrO_2-SnO_2 core-shell

2.25 g $SnCl_2$.2H_2O was dissolved in 30 ml of deionized water, and. 10 ml of H_2O_2 (%30 v/v) was added into solution. After 30 min stirring, 0.3g nano-ZrO_2 was added under stirring at room temperature. The pH of above suspension was increased to 10 by addition 0.2 M NaOH solution under stirring. The mixture was transferred into a Teflon-lined stainless steel autoclave. Hydrothermal treatments were carried out at 120 ºC for 24h. After that, the autoclave was allowed to cool down naturally. White precipitates were collected and washed with deionized water and ethanol several times to remove impurities. Finally, the precipitates were dried at room temperature.[34].

$$SnCl_2 + 2 H_2O_2 \Rightarrow Sn(OH)_4 + Cl_2$$
$$Sn(OH)_4 \Rightarrow SnO_2 + 2H_2O$$
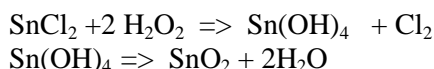
2.3 Photo-catalytic degradation Experiments

Congo Red(CR) was chosen as a model of water pollution to evaluate the photocatalytic behavior of the ZrO_2-SnO_2 Core shell NPs. Photo-degradation of 10 parts per million (ppm) Congo red solutions were employed to assign the performance of, ZrO_2- SnO_2 Core shell NPs as a photo-catalysts. For each condition, 0.05 g of photocatalyst was dispersed into 100 ml of 10 ppm CR aqueous solution. The CR solution was mixed and ensured full suspension of the particles. The photocatalytic reaction was conducted under UV light from a single 15W UV tube at 254 nm positioned above the liquid surface at RT. The distance between the lamp and the base of the beaker was 10 cm. Each experiment was conducted for 30 min with 5ml sample aliquots extracted every 5 min, a sample of reaction suspension was centrifuged at 3000 rpm to remove the photocatalyst. The solution absorbance was measured using UV–Vis spectrophotometer (U-3010, HITACHI) at the maximum absorption band 502 nm (λ_{max} of CR).

Photo-catalytic degradation (PD) % was calculated using the formula (1):

$$\%PD = \left[\frac{Ao-At}{Ao}\right] \times 100 = \left[\frac{C_0-C_t}{C_0}\right] \times 100 \tag{1}$$

where C0, Ct, A0, and At are the initial concentration of the azo dye , contaminant concentration after irradiation time t, initial absorbance, and final absorbance of the sample after irradiation time t, respectively [35]

Adsorption capacity X_m(mg/g) was calculated using the formula (2):

$$X_m = \frac{(C_0 - C_t) \times V}{W} \tag{2}$$

3. Results and Discussion

3.1 FT-IR Analysis

The FT-IR spectra of ZrO2 and ZrO_2-SnO_2 core-shell NPs are shown in Fig. 1a, b in the wave-number range from 4000 to 400 cm^{-1}. In Fig 1a, the broad absorption around 3439 cm^{-1} has been assigned to the OH symmetry and asymmetry stretching vibration of residue water molecules and Zr-O-H stretching g of surface group. The peak at 1632 cm^{-1} resulted from bending vibration of the adsorbed H_2O molecules. The peak at 1499 cm^{-1} can to be caused from Zr-O-H bending of surface groups. The peaks at 752, 662, 575, 499 and 419 cm^{-1} can be attributed to stretching and bending vibrations of the O-Zr-O and Zr-O-Zr bonds[36]In Fig 1b, the peak at 3413 cm^{-1} is resulted from the OH symmetry and asymmetry stretching vibration of water molecules and M-O-H stretching g of surface group. The peak at 1624 cm^{-1} is assigned to bending vibration of the adsorbed H_2O molecules. The peak at 1421 cm^{-1} can to be caused from M-O-H bending of surface groups. The wide peak between 1000-400 cm^{-1} has been assigned to the vibrations of the O-M-O and M-O-M(M= Zr and Sn) bonds[37-39].
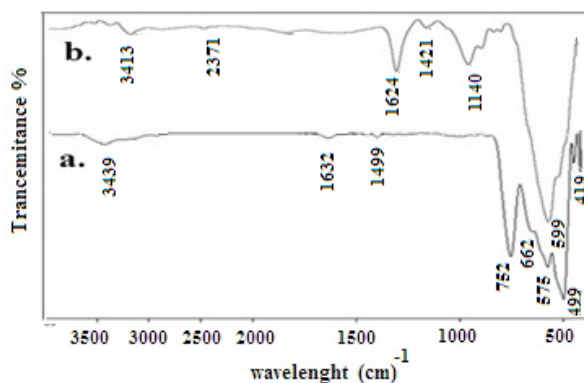

Fig. 1. FT-IR Spectra of (a) NanoZrO2 and (b)Nano ZrO_2-SnO_2

3.2 Crystallite Phase Characterization

X-ray diffraction (XRD) at 40Kv and 30 mA was applied to identify crystalline phases and to calculate crystalline sizes. The XRD patterns of the ZrO2 and ZrO_2-SnO_2 core-shell NPs are shown in Fig. 2.In Fig.2a the peaks indicate the respective Joint Committee on Powder Diffraction Standards (JCPDS) card no. 37-1484 for monoclinic structure of ZrO_2 with space group P21/c. The diffraction peaks at angles (2θ) of 24.20 , 24.60 , 28.32 , 31.58 , 34.30, 35.95 , 40.80 , 49.38 , 50.27 ,55.58, and 59.98 attributed to(011), (110), (111), (-111), (002), (200), (211), (022), (220), (013) , and (-131) crystal planes of the monoclinic zirconium dioxide.

In Fig2b, the overall crystalline structure shows a monoclinic of zirconium dioxide with referred (111) and (-111) orientations at 2θ= 28.32 and 31.58 and a tetragonal tin dioxide with referred (110), (101), (200) and (211) orientations at 2θ= 26.67, 33.90, 37.97 and 51.89.
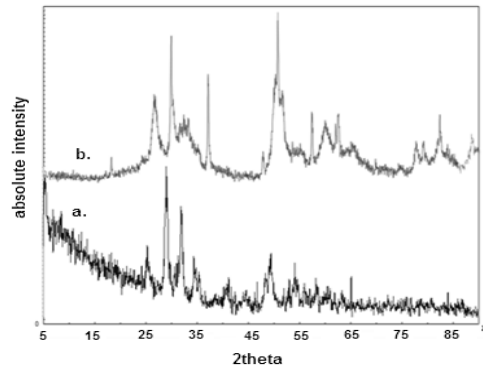
Fig. 2. XRD patterns of (a) NanoZrO2 and (b) Nano ZrO$_2$- SnO$_2$

The average crystallite size of NPs Dv was calculated based upon the XRD patterns for quantitative purpose using the Debye- Scherer equation(3):

$$Dv = \frac{K\lambda}{\beta \cos\theta} \qquad (3)$$

where *Dv* is the "volume weighted" crystallite size = ¾ d (crystallite diameter) K is the "Scherer constant" (around 0.94) , λ is the CuKα = 1.541 Å, θ is the Bragg angle for the peak at 2 θ, β is the FWHM for a Gaussian shaped peak [40].

The value of the dislocation density (δ) of matter is a measure of amount of defects in the crystal [41, 42]. The dislocation density can be defined as the length of dislocation lines per unit volume, and is calculated using the equation (4):

$$\delta = \frac{1}{D_v{}^2} \qquad (4)$$

The micro-strain (ε) of the investigated samples was estimated [43, 44], using the formula (5):

$$\varepsilon = \frac{\beta cos\theta}{4} \qquad (5)$$

The calculated values of structural parameters of the ZrO2 and ZrO$_2$- SnO$_2$ core-shell NPs are depicted in Table (1).

Table.1 Structural parameters of ZrO$_2$-ZnO and ZnO-ZrO$_2$

Nano material	Average crystallite Size (nm)	Dislocation density x10^{14} (line/m^2)	Micro-strain [line^{-2}m^{-4}] x10^{-4}
NanoZrO$_2$	22.4	19.93	16.17
NanoZrO$_2$- SnO$_2$	23.1	18.74	15.68

3.3 Morphological Observations and elemental Analysis

Fig.3 shows the FESEM and particle size histogram of nano- ZrO$_2$. As shown, the ZrO$_2$ nanoparticles consist of monoclinic morphology with the less agglomeration of the particles. The mean particles is in the range of 50-80 nm.
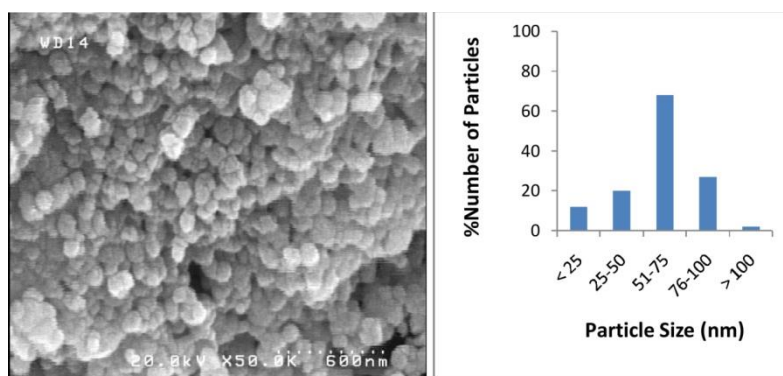
Fig. 3. FESEM photograph and Particle size histogram of Nano-ZrO₂

Fig.4 presents the FESEM images of the ZrO_2-SnO_2 core-shell NPs and the corresponding histogram of the particlesize distribution. As shown, NPs comprised of platelet like nano particles. The mean particles is in the range of 75-100 nm.
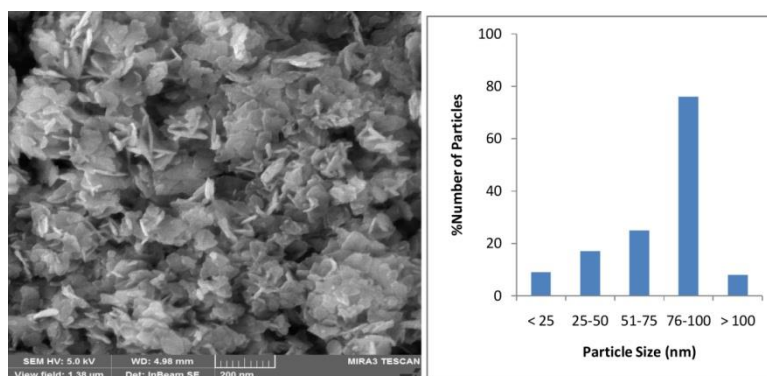

Fig. 4. FESEM photograph and Particle size histogram of ZrO₂-SnO₂ core-shell NPs

Elemental analysis using Emission X-ray dispersive analyses (EDX) of the samples are shown in Table 2 giving the percentage elemental ratio of nano-ZrO_2 and ZrO_2-SnO_2core-shell NPs.

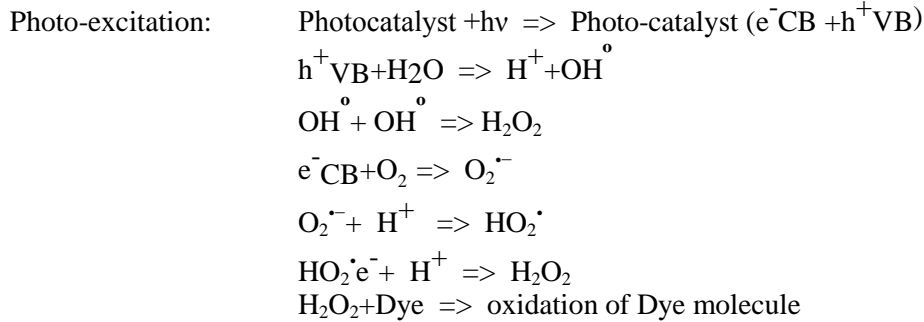*Table2. EDX quantification of the percentage ratio of Sn , Zr and Oxygen*

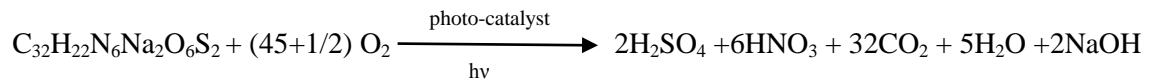| Element	Nano-ZrO₂		ZrO₂-SnO₂core-shell	
	W %	A %	W %	A %
Sn	-	-	42.43	19.51
Zr	76.16	34.32	34.21	20.17
O	23.84	65.59	21. 35	59.83

3.4 Photodegradation Analysis

In Fig. 5a, is shown the photo-catalytic degradation efficiency of CR using nano-ZrO_2 and ZrO_2-SnO_2core-shell NPs under UV light irradiation. The blank experiment without catalyst was rarely decomposited with about 3% of degradation of CR within 30 min of UV irradiation.

It could be found that CR is hardly photo-decomposed by using nano ZrO_2 because the band gap energy of ZrO_2 is about 5 eV. The very high efficiency of degradation of CR could be seen on the ZrO_2-SnO_2core-shell photocatalyst, it approaches to 96% after 30 min .The ZrO_2-SnO_2core-shell was exhibited very high photo-catalytic performance than the nano ZrO2

photocatalyst. The composite of semiconductors is one of the ways to improve the photo-catalytic property. Photocatalytic reaction is initiated when a photo-excited electron is promoted from the filled VB of semiconductor photocatalyst (SC) to the empty CB as the absorbed photon energy, hν, equals or exceeds the band-gap of the semiconductor photocatalyst leaving behind a hole in the VB. Thus in concert, electron and hole pair (e−–h+) is generated. The following chain reactions have been widely postulated [45].

Photo-excitation: Photocatalyst $+h\nu$ => Photo-catalyst $(e^-CB + h^+VB)$

$h^+VB + H_2O$ => $H^+ + OH^o$

$OH^o + OH^o$ => H_2O_2

$e^-CB + O_2$ => $O_2^{\cdot -}$

$O_2^{\cdot -} + H^+$ => $HO_2^{\cdot}$

$HO_2^{\cdot}e^- + H^+$ => H_2O_2

$H_2O_2 + Dye$ => oxidation of Dye molecule

Both the oxidation and reduction can take place at the surface of the photo-excited semiconductor photocatalyst. Recombination between electron and hole occurs unless oxygen is available to scavenge the electrons to form superoxides $(O_2^{\cdot -})$, its protonated form the hydroperoxyl radical $(HO_2^{\cdot})$ and subsequently H_2O_2 [6]. As shown the below reaction, the products of photo-degradation of CR are safety for environment

$$C_{32}H_{22}N_6Na_2O_6S_2 + (45+1/2)\ O_2 \xrightarrow[h\nu]{photo\text{-}catalyst} 2H_2SO_4 + 6HNO_3 + 32CO_2 + 5H_2O + 2NaOH$$

According the equation (2), the maximum Adsorption capacity X_m of nano-ZrO_2 and ZrO_2-SnO_2 core–Shell NPs was calculated 2.2 and 19.2 mg/g respectively.

3.5 The kinetic study of photodegradation

The Langmuir-Hinshelwood model can be used to describe the relationship between the rates of the photocatalytic degradation of dye in the presence of nano-ZrO_2 or ZrO_2-SnO_2 core-shell NPs as a function of irradiation time. The rate equation is used in the relation (6):

$$\frac{-dC}{dt} = \frac{k_{L-H}K_{ad}\ C}{1+\ K_{ad}C}(6)$$

where K_{ad} is the adsorption coefficient of the reactant on nano-ZrO_2 or ZrO_2-SnO_2 core-shell NPs, k_{L-H} is the reaction rate constant and C_t is the concentration at time t. Then, by integration of Equation 6:

$$Ln\left(\frac{C_0}{Ct}\right) = K(C_t - C_0) + k_{L-H}K_{ad}t \qquad (7)$$

where C_0 is the initial concentration

For pseudo-first-order reaction $K_{ad}C$ is very small compared to 1 in the denominator of Equation 6, so it is simplified and integrated to be:

$$Ln\left(\frac{C_0}{Ct}\right) = k_{L-H}K_{ad}t = kt \qquad (8)$$

where $k = k_{L-H}K_{ad}$ is the pseudo-first-order reaction rate constant, and the half-life time $t(1/2)$ can be calculated using the following expression:

$$t_{1/2} = \frac{0.693}{k} \tag{9}$$

As it is well accepted that the photodegradation of CR solution accords with a pseudo first order kinetic [46, 47] the relationship between - $Ln(C_t/C_0)$ and reaction time were plotted and shown in Fig. 5b.The rate constant is the slope of the straight line in Fig. 5b. Equation 9 was used to calculate the half-life time for the photocatalytic degradation of CR by nano-ZrO_2 or ZrO_2-SnO_2 core-shell NPs. The kinetic data values are summarized in Table 3.

Table 3.The Kinetic parameters of photocatalytic degradation of CD by Nano-ZrO_2 and ZrO_2-SnO_2

Photocatalyst	Rate constant (min)	Half-life time (min^{-1})	Standard deviation (R^2)
Nano-ZrO_2	0.003	231	0.987
ZrO_2-SnO_2core-shell	0.106	6.5	0.990

The results, given in Fig.5c, demonstrate that the ZrO_2-SnO_2 core-shell NPs can serve as highly effective and convenient recyclable photo-catalysts. After 3cycles, only a slight decrease in the photodecomposition rate was observed
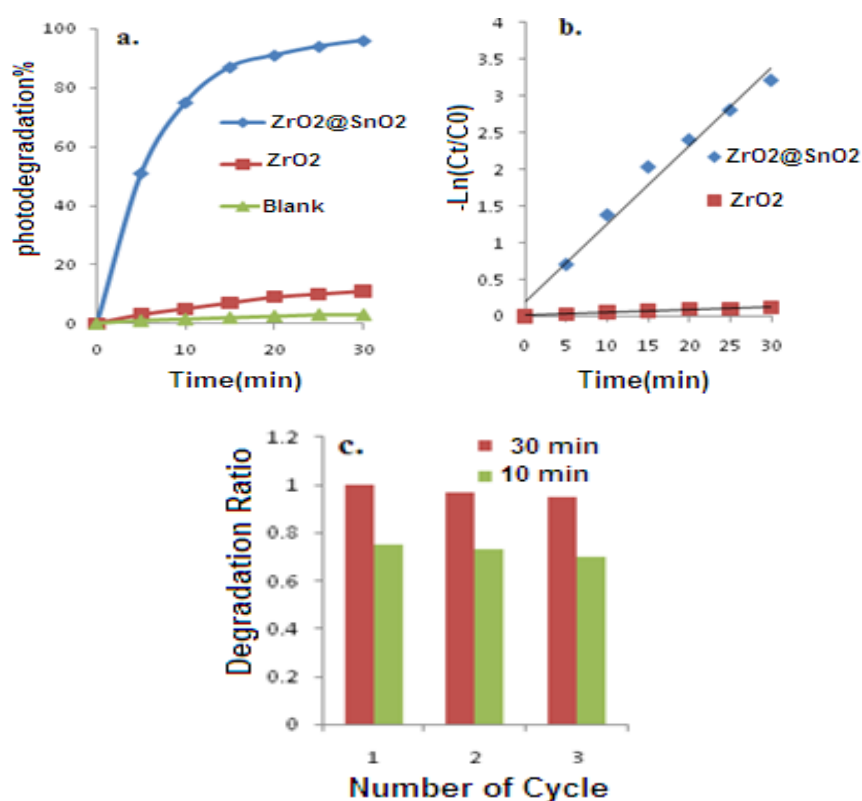

Fig.5. a) Plot of photo degradation of CR versus reaction time, b) Relationship between -$Ln(C_t/C_0)$ and reaction time for photodegradation of CR, c) Recyclability of ZrO_2-SnO_2 core-shell as photocatalyst in degradation of CD.

4. Conclusions

ZrO_2-coated SnO_2 has been developed by using hydrothermal process The analysis of XRD revealed that the ZrO_2 possess monoclinic phase and the SnO_2 shows well crystalline tetragonal phase. , the mean of calculated value as crystallite size of nano-ZrO_2 and ZrO_2-SnO_2Core–Shell NPs was obtained 22.4 and 23.1 nm respectively. The FESEM analysis showed

88

monoclinic morphology and platelet like of nano-ZrO_2 and ZrO_2-SnO_2 core–shell NPs respectively.

The very high efficiency of degradation of CR could be seen on the ZrO_2-SnO_2core-shell photocatalyst. The reason of the photo-degradation performance of core-shell results from the band gap of ZrO_2-SnO_2core-shell NPs. The combination ZrO_2 and SnO_2 as core shell with different band gaps forms hetero-junctions in photocatalytic systems

Acknowledgment

References

[1] M.S. Diaz-Cruz, D. Barcelo, Chemosphere **72** , 333(2008)

[2] S. Merouani, O. Hamdaoui, F. Saoudi, M.S. Chiha, Chemical Engineering Journal **158**, 550 (2010)

[3] M.F. Abdel-Messih, M.A. Ahmed, Ahmed Shebl El-Sayed, J. Photochemistry and Photobiology A: Chemistry **260**, 1 (2013)

[4] Rais Ahmad, Rajeev Kumar, Applied Surface Science **257**, 1628(2010)

[5] W. Cun, Z. Jincai, W. Xinming, M. Bixian, S. Guoying, P. Ping'an, F. Jiamo, Appl. Catal. B **39**, 269(2002).

[6] H.R. Pouretedal, Z. Tofangsazi, M.H. Keshavarz, Journal of Alloys and Compounds **513**, 359(2012)

[7] C. Karunakaran, S. Senthilvelan, J. Mol. Catal. A 233 , 1–8(2005).

[8] N. Smirnova, Y. Gnatyuk, A. Eremenko, G. Kolbasov, V. Vorobetz, I. Kolbasova, O. Linyucheva, Int. J. Photoenergy **1–6**, 2006 (2006)

[9] S.R. Dhage, S.P. Gaikwad, V. Samuel, V. Ravi, Bull. Mater. Sci. 27 , 221–222 (2004)

[10] A.E. Kandjani, P. Salehpoor, M.F. Tabriz, N.A. Arefian, M.R. Vaezi, Mater. Sci.-Poland **28**, 377 (2010)

[11] M.E. Manřııquez, T. Lˇıopez, R. Gˇı omez, J. Navarrete, J. Mol. Catal. A **220**, 229(2004)

[12] S.C. Hayden, N.K. Allam, M.A. El-Sayed, Journal of the American Chemical Society **132**, 14406 (2010)

[13] H. Kim, J. Kim, W. Kim, W. Choi, Journal of Physical Chemistry C **115**, 9797(2011)

[14] F. Fresno, M.D. Hernandez-Alonso, D. Tudela, J.M. Coronado, J. Soria, Applied Catalysis B: Environmental **84**, 598(2008)

[15] D.R. Baker, P.V. Kamat, Advanced Functional Materials **19**, 805 (2009).

[16] Q. Zhang, W. Fan, L. Gao, Applied Catalysis B: Environmental **76**, 168(2007).

[17] G. Yang, Z. Yan, T. Xiao, Applied Surface Science **258**, 8704(2012)

[18] J .Kong, H, Deng, P. Yanga,, J. Chu,.Mater. Chem. Phys; **114**, 854(2009)

[19] X. Zhong, B. Yang, X. Zhang, J. Jia, G. Yi..Particuology, **10**, 365(2012).

[20] Y. Liu, W. Yang, Z. Dai, H.Chen, X. Yang, D. Hou, .MaterChemPhys, **112**, 381 (2008)

[21] T. Krishnakumar, R. Jayaprakash, N. Pinna, V. N. Singh, B. R. Mehta, A. R. Phani.Mater Lett, **63**, 242(2009)

[22] T. Krishnakumar, R. Jayaprakash, M. Parthibavarman, A. R.Phani, V. N. Singh, B. R .Mehta, MaterLett, **63**, 896(2009);.

[23] C. Fu, J. Wang, M. Yang, X. Su, J. Xu, B. Jiang.J. Non-Cryst Solids , **357**, 1172(2011).

[24] M. A. Gondala, Q. A. Drmosh, T. A. Saleh, Appl. Surf. Sic, **256**, 7067 (2010).

[25] A. A. Firooz, A. R. Mahjoub, A. A. Khodadadi, .Mater Lett , **62**, 1789(2008).

[26] S. Supothina, R. Rattanakam, S. Vichaphund, P. Thavorniti. J. Euro. Ceram. Soc, **31**, 2453 (2011)

[27] S. M. Sedghi, Y. Mortazavi, A. Khodadadi. SensorsActuatorsB, 1**45**, 7 (2010).

[28] M. Aziz, S. S. Abbas,W. Rosemaria W. Baharom, Materials Letters **91**,31(2013).

[29] J.M.E. Matos, , F.M. Anjos Júnior, L.S. Cavalcante, V. Santos, S.H. Leal, L.S. Santos Júnior, M.R.M.C. Santos, E. Longo, Materials Chemistry and Physics **117**, 455(2009)

[30] Y-Q. Song, D-H. He, B-Q. Xu, Applied Catalysis A: General **337**, 19(2008)

[31] Y. Chang, X. Li, Trans. Nonferrous Met.. SOC. China **16**, 332(2006)

[32] C. M Fiona. Woudenberg, F. C. Wiebke. S. E. J. Elshof, H. Verweij, J. Am. Ceram. Soc., **87**,1430 (2004)

[33] S. Wang, , X. Li, Y. Zhai, K. Wang, Powder Technology **168**, 53(2006)

[34] S. K. Tripathy, T. Sahoo, H. Lee, Y-T. Yu, Materials Letters **61**, 4690 (2007)

[35] A. Nezamzadeh-Ejhieha,, M. Bahrami, Desalination and Water Treatment, **55**, 1096 (2015)

[36] J.M.E. Matos, F.M. Anjos Júnior, L.S. Cavalcante, V. Santos, S.H. Leal, L.S. Santos Júnior, M.R.M.C. Santos, E. Longo, Materials Chemistry and Physics **117**, 455(2009)

[37] M.F. Abdel-Messih, M.A. Ahmed, A. S. El-Sayed, Journal of Photochemistry and Photobiology A: Chemistry **260**, 1(2013)

[38] S. Emiroglu, N. Bârsan, U . Weimar, V. Hoffmann. Thin Solid Films ,**391**, 176(2001).

[39] P .Manjula, L . Satyanarayana, Y. Swarnalatha, S. V. Manorama, Sens. Actuators B Chem , **138**, 28(2009).

[40] H.P.Klug, L.E. Alexander, X-ray Diffraction Procedures, Wiley, New York, (1954).

[41] A. Kropid owska, J. Chojnacki, A. Fahmi, B. Becker, Dalton Trans. **47**, 6825 (2008).

[42] V. Bilgin, S. Kose, F. Atay, I. Akyuz, Mater. Chem. Phys. **94**, 103 (2005).

[43] Z.R. Khan, M. Zulfequar, Mohd. Shahid Khan, Mater. Sci. Eng. B **174**, 145 (2010).

[44] A. A. AKL, S. A. ALY, H. HOWARI, Chalcogenide Letters, **13**, 247 (2016)

[45] K. Rajeshwar, M.E. Osugi, W. Chanmanee, C.R. Chenthamarakshan, M.V.B. Zanoni, P. Kajitvichyanukul, R. Krishnan-Ayer, J. Photochem. Photobiol. C **9**,171. (2008)

[46] J. Tian, L. Chen, Y. Yin, X. Wang, J. Dai, Z. Zhu, X. Liu, P. Wu, Surf. Coat. Technol. **204**, 205 (2009)

[47] M.A. Mahmoud, A. Poncheri, Y. Badr, M.G. A. El Wahed, , South African Journal of Science **105**,299 (2009)